COGNITIVE NEUROSCIENCE

Synaptic rearrangement of NMDA receptors controls memory engram formation and malleability in the cortex

Benjamin Bessières[1], Julien Dupuis[2], Laurent Groc[2], Bruno Bontempi[1,3]*†, Olivier Nicole[1,2]*†

Initially hippocampal dependent, memory representations rely on a broadly distributed cortical network as they mature over time. How these cortical engrams acquire stability during systems-level memory consolidation without compromising their dynamic nature remains unclear. We identified a highly responsive "consolidation switch" in the synaptic composition of *N*-methyl-D-aspartate receptors (NMDARs), which dictates the progressive embedding and persistence of enduring memories in the rat cortex. Cortical GluN2B subunit–containing NMDARs were preferentially recruited upon encoding of associative olfactory memory to support neuronal allocation of memory engrams. As consolidation proceeds, a learning-induced redistribution of GluN2B subunit–containing NMDARs outward synapses increased synaptic GluN2A subunit contribution and enabled stabilization of remote memories. In contrast, synaptic reincorporation of GluN2B subunits occurred during subsequent forgetting. By manipulating the surface distribution of GluN2A and GluN2B subunit–containing NMDARs at cortical synapses, we uncovered that the rearrangement of GluN2B-containing NMDARs constitutes an essential tuning mechanism that determines the fate of cortical memory engrams and controls their malleability.

INTRODUCTION

Initially labile, memories for facts and events undergo a process termed systems consolidation via which they acquire stability and persistence over time (*1*–*4*). This time-dependent process requires the hippocampus that operates as a crucial consolidation organizing device with extrahippocampal regions, namely cortical regions, becoming progressively capable of storing and retrieving enduring memories independently (*1*–*5*). Such remote memories become embedded into distributed cortical networks that host the so-called memory engram cells that are thought to constitute the physical substrate of a memory (*6*). Neurons compete for this privilege, and only those with advantageous excitability properties are preferentially allocated to the memory engram (*7*, *8*). We previously identified early cortical tagging of eligible neurons as a prerequisite for the formation of remote memory and suggested that tagged neurons upon encoding may serve as the scaffolding to support the progressive hippocampal-driven embedding of memory engrams into cortical networks (*9*). Yet, the cellular and molecular events governing the progressive maturation of cortical engram cells from a silent to an active form capable of expressing the dynamic nature of memory representations have remained elusive.

The traditional assumption that persisting memories remain essentially unmodifiable is being challenged in view of accumulating psychological accounts showing that consolidated engrams may continue to change as a result of experience, a concept referred to as memory malleability (*10*). Curiously, current models of systems consolidation do not adequately capture the dynamic nature of remote memories and fail to provide a unifying framework accounting for the available experimental reports (*11*). This is mainly because of a lack of evidence for a supportive mechanism at the neuronal level capable of dynamically arbitrating the competition between persistence, updating and forgetting of cortical engrams.

Enhanced synaptic strength between interconnected neurons recruited upon memory encoding is thought to form the synaptic correlate for remote memory formation (*12*, *13*). Within this framework, the plasticity-stability continuum of synaptic connectivity implies a delicate balance capable of accommodating ongoing storage of new information while protecting older memories against potential interferences (*14*, *15*). As fundamental coincidence detectors of synaptic activity necessary for the induction of synaptic plasticity (*16*), postsynaptic *N*-methyl-D-aspartate receptors (NMDARs) are considered a crucial component of this regulatory balance. Spatiotemporal rearrangements in the synaptic organization of these receptors have recently emerged as a key feature regulating the efficacy of excitatory synaptic transmission (*17*) and supporting memory processing in the hippocampus (*18*). Notably, activity-dependent surface trafficking–based adjustments in the synaptic content of the two predominant GluN2A and GluN2B subunit–containing NMDARs expressed in the adult forebrain were found to modulate the initiation of functional and structural synaptic adaptations (*17*, *19*–*21*). Whether such changes at the nanoscale level adequately support the dynamics of cortical engrams is unknown. We therefore set out to explore whether synaptic redistributions of cortical GluN2A and GluN2B subunit–containing NMDARs occur during the course of systems consolidation and constitute an essential gating mechanism for cortical synapses to undergo stability or plasticity, thereby fulfilling the intrinsic requirements of remote memories, which are persistence (recollecting), malleability (updating), and forgetting (transience) (*22*).

RESULTS

Functional rearrangement of NMDAR subtypes at cortical synapses is required for remote memory formation

To unravel the reorganization of cortical GluN2A and GluN2B subunit–containing NMDARs as memories mature during the course

[1]Institut des Maladies Neurodégénératives, CNRS UMR 5293, Université de Bordeaux, Bordeaux 33000, France. [2]Institut Interdisciplinaire de Neurosciences, CNRS UMR 5297, Université de Bordeaux, Bordeaux 33000, France. [3]Institut de Neurosciences Cognitives et Intégratives d'Aquitaine, CNRS UMR 5287, Université de Bordeaux, Bordeaux 33000, France.
*Corresponding author. Email: bruno.bontempi@u-bordeaux.fr (B.Bo.); olivier.nicole@u-bordeaux.fr (O.N.)
†These authors contributed equally to this work.

of systems-level memory consolidation, we trained rats in the social transmission of food preference (STFP) paradigm, which involves an ethologically based form of associative olfactory memory (*23*). In this hippocampal-dependent task (*9*), rats learn within one single-interaction session about the safety of potential food sources by sampling the odor of those sources on the breath of conspecifics (*23*). After interacting with a demonstrator rat fed with cumin-powdered food, experimental rats reversed their innate preference for thyme and preferentially ate cumin when given a choice between these two flavors (Fig. 1A). The acquired associative olfactory memory for cumin was robust and long-lasting as it remained stable over 30 days after encoding, and a delay as long as 60 days was required to induce notable forgetting (Fig. 1A and fig. S1). Because encoding in this paradigm occurs rapidly without repeated training sessions (*9*, *23*), we were able to dissect the time course of NMDAR reorganization in cortical regions involved in memory processing. We generated postsynaptic density (PSD)–enriched membrane fractions obtained from the orbitofrontal cortex (OFC), which constitutes a central hub within the distributed cortical network underlying remote memory formation in the STFP paradigm (fig. S2) (*24*). We observed a time-dependent shift in the subunit composition of synaptic NMDARs as memories matured over time (Fig. 1B and fig. S3). Relative to day 1, the GluN2A-/GluN2B-containing NMDAR ratio in the OFC increased at day 15 following social interaction (as a result of reduced GluN2B subunit expression; fig. S3, D and E), suggesting an enhanced contribution of GluN2A-NMDARs at this long-term delay. This signature in the NMDAR subunit composition persisted at day 30 (Fig. 1B and fig. S3, D and E), a remote delay for which retrieval of consolidated memories is heavily dependent on the OFC (fig. S2, B and C) (*9*). In contrast, in rats experiencing substantial forgetting at the longer delay of 60 days, the balance in GluN2B- and GluN2A-NMDARs fluctuated again and tilted in favor of GluN2B-NMDARs as shown by a decreased GluN2A/GluN2B expression ratio (Fig. 1B and fig. S3, D and E). Thus, successful retrieval of "corticalized" memories appears to rely on the contribution of GluN2A-containing NMDARs in the OFC at days 15 and 30, while memory degradation is associated with an enhanced participation of GluN2B-containing NMDARs at day 60.

We next examined the specificity of these time-dependent changes in the composition of synaptic NMDARs in the cortex. Not all cortical regions are expected to be disproportionally involved in processing nonspatial associative olfactory information either

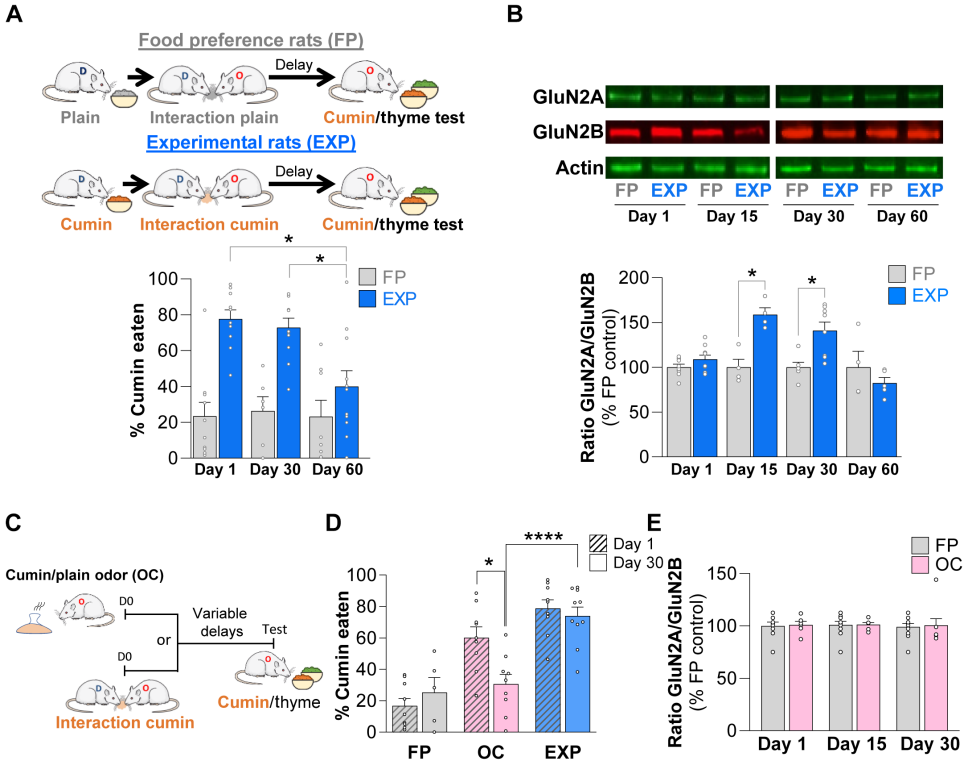

Fig. 1. Time-dependent rearrangement of synaptic GluN2A and GluN2B subunit–containing NMDARs during systems-level consolidation of remote associative olfactory memory. (**A**) Experimental design (top) and time course of memory formation (bottom). Performance of EXP rats was robust and long-lasting with forgetting occurring only after 60 days (group × delay interaction: $F_{2,50} = 3.52$; $P < 0.05$); *$P < 0.05$. (**B**) Immunoblots (top) and quantitative analysis (bottom) of NMDAR subunit expression in PSD-enriched membrane fractions from the OFC of FP and EXP rats. A progressive increase in the GluN2A/GluN2B ratio occurred as memory consolidated in the OFC of EXP rats (day 15, long-term memory; day 30, remote memory). At day 60, memory forgetting was associated with an increased contribution of GluN2B-containing NMDARs (group × delay interaction: $F_{3,40} = 7.20$; $P < 0.001$); *$P < 0.05$. (**C**) Experimental design investigating memory persistence. EXP rats interacted socially with a demonstrator fed with cumin-flavored chow. Odor control (OC) rats were only able to smell cumin from a jar. (**D**) Enhanced preference for cumin-flavored food remained stable over 30 days in EXP rats but faded over the same time period in OC rats (group × delay interaction: $F_{2,45} = 4.44$; $P < 0.05$). Performance of OC rats at day 30 was similar to that of FP controls, which interacted with a demonstrator fed with plain food. (**E**) Quantitative analysis of NMDAR subunit expression in PSD-enriched membrane fractions from the OFC of FP and OC rats tested at various intervals (days 1, 15, and 30) following social interaction. No redistribution of synaptic GluN2A and GluN2B subunits occurred over time in OC rats (group × delay interaction: $F_{2,43} = 0.013$; $P > 0.98$, NS). *$P < 0.05$, ****$P < 0.0001$. (A), (B), (D), and (E), $n = 4$ to 11 rats per group.

recently or remotely. One such region is the parietal cortex, which has been shown to be predominantly involved in processing and retrieving remote spatial information (*25*). Accordingly, no significant time-dependent changes in synaptic NMDAR subunit composition was observed in this cortical region, contrasting with those observed in the OFC (fig. S4). Two memory components, namely olfactory and associative, act in concert to support performance in the STFP paradigm. Because olfactory memory (elicited solely by a cumin flavor) is not as persistent as associative olfactory memory, which requires social encounter with a demonstrator rat upon encoding (Fig. 1, C to E, and fig. S5) (*26*, *27*), we expected a differential outcome on the NMDAR subunit reorganization in the OFC over time. Consistent with this prediction, only successful consolidation of a remotely acquired associative memory, but not a faded olfactory memory or the absence of a memory association in food preference (FP) controls, was associated with an increased GluN2A/GluN2B expression ratio at synapses of OFC neurons (Fig. 1, C to E, and fig. S5). Collectively, these findings indicate that the consolidation-induced switch in the subunit composition of cortical NMDARs is region-, memory-, and persistence-specific. Since Western blot analysis cannot distinguish between engram and non-engram cells, we next applied an electrophysiological approach to evaluate whether this molecular switch determines the functional properties of NMDAR-mediated excitatory postsynaptic currents (EPSCs) specifically in engram cells. OFC neurons of rats tested either 1 day (recent memory) or 30 days (remote memory) after social interaction (fig. S6) were infected with lentiviruses expressing an enhanced form of the synaptic activity–responsive element (E-SARE) within the immediate early gene *Arc* promoter (Fig. 2A and fig. S7) (*28*). This dual fluorescent reporter system enabled selective whole-cell patch-clamp recordings from infected neurons expressing the red fluorescent protein (RFP) that were either activated [destabilized green fluorescent protein (dGFP)–positive] or nonactivated (dGFP-negative) upon memory retrieval. The inhibition magnitude of NMDAR-mediated EPSCs by the selective GluN2B subunit–containing NMDAR antagonist Ro 25-6981 did not differ when comparing task-activated ($dGFP^+/RFP^+$) and nonactivated neurons ($dGFP^-/RFP^+$) 1 day after social interaction (decay time: Fig. 2B and fig. S8A; amplitude fig. S9, A and B). In contrast, at day 30, Ro 25-6981 yielded a weaker inhibition of NMDAR-EPSCs in activated neurons compared to nonactivated neurons (decay time: Fig. 2B and fig. S8B; amplitude: fig. S9, C and D), thereby confirming a decrease in the contribution of GluN2B-containing NMDARs during maturation of the cortical engram without affecting the amplitude of NMDA-mediated EPSCs [fig. S9, E and F; see also (*13*)]. To test whether this molecular rearrangement is necessary for the establishment of a consolidated remote memory in the cortex, we selectively disabled GluN2A and GluN2B subunit–containing NMDARs in the OFC during two post-learning time windows: an early remodeling period (from days 1 to 11) critically dependent on coordinated hippocampal-cortical interactions and a late (from days 16 to 26) hippocampal-independent stabilization period, which relies heavily on cortical-cortical interactions to strengthen reorganized cortical networks (Fig. 3A) (*9*). The GluN2B-containing NMDAR selective antagonist ifenprodil impaired remote memory retrieval probed at day 30 only when administered during the early remodeling, but not late stabilization phase, of memory maturation (Fig. 3B and fig. S10, A and B). In sharp contrast, antagonizing GluN2A-containing NMDARs with TCN-201 was effective in abolishing remote memory retrieval only when delivered during the late stabilization phase of memory consolidation (Fig. 3B and fig. S10, A and B). Consistent with this, intra-OFC infusions of the nonselective NMDAR

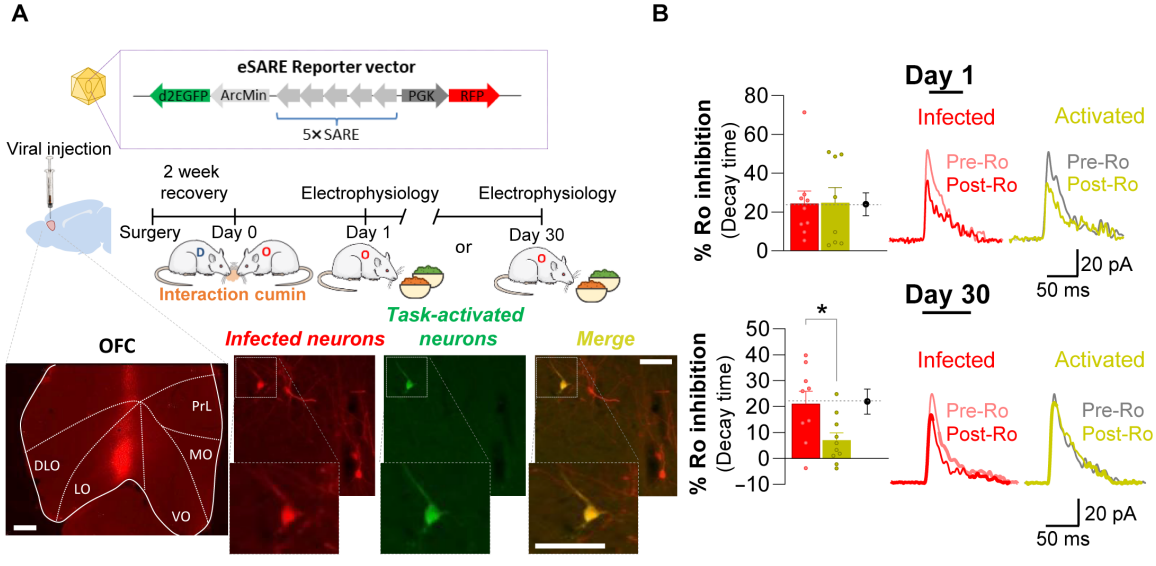

Fig. 2. Characterization of the NMDAR-mediated EPSCs in engram neurons recorded upon recent and remote retrieval of associative olfactory memory. (**A**) Neurons recruited upon retrieval at either recent (day 1) or remote (day 30) memory retrieval (top) were tracked using E-SARE virus infusions (red) into the lateral subdivision (LO) of the OFC (bottom left; scale bar, 500 μm). E-SARE–infected (red) and -task–activated (Arc^+, green) neurons (bottom right) are shown. Scale bars, 50 μm; inset, 50 μm. (**B**) Spontaneous NMDAR-mediated EPSCs of task-activated and E-SARE–infected neurons in the OFC were similarly inhibited by Ro 25-6981 at day 1 (top left, $t_{15} = 0.05$; $P = 0.96$, NS); at day 30, only task-activated neurons were relatively insensitive (bottom left, reduced inhibition, $t_{18} = 2.66$; $P = 0.02$); infected (Arc^-) neurons were unaffected regardless of the delay; noninfected adjacent neurons (dotted line) served as control; $^*P < 0.05$, 8 to 10 neurons were recorded. Representative NMDAR EPSC traces of E-SARE–infected (red) and -task–activated (yellow) neurons (top and bottom right) are shown before and after Ro 25-6981 incubation.

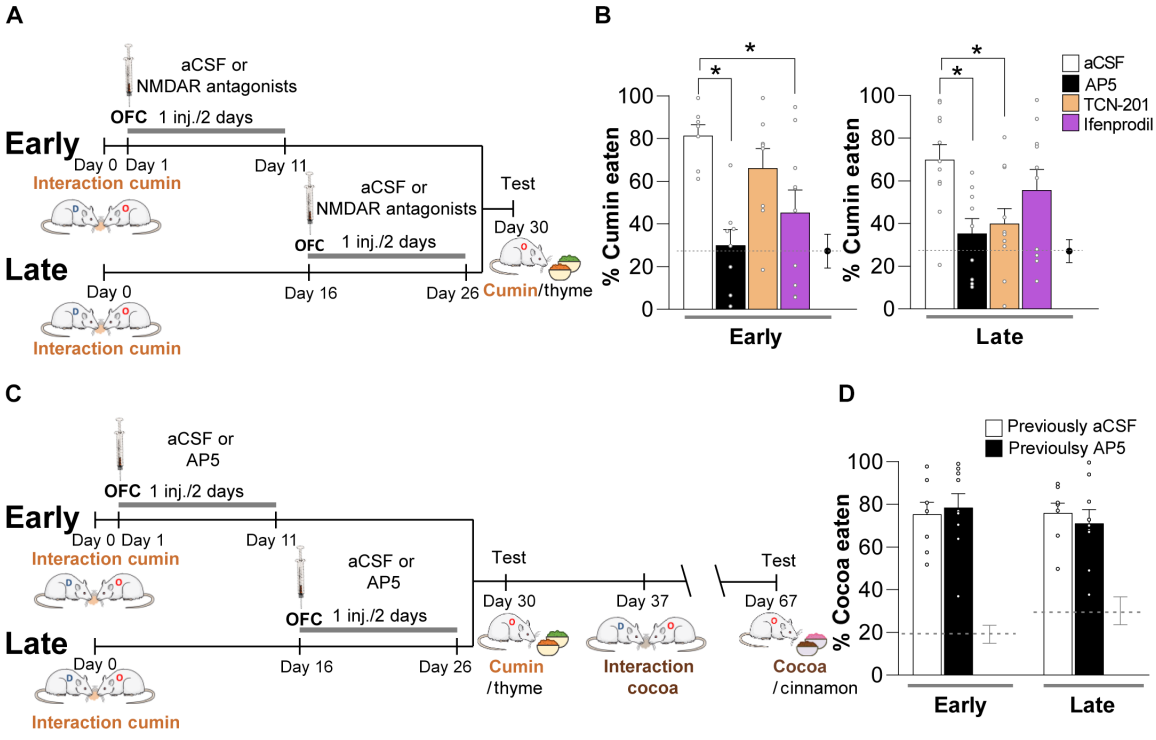

Fig. 3. Time-dependent rearrangement of synaptic GluN2A and GluN2B subunit–containing NMDARs is required for the formation of remote associative olfactory memory in the OFC. (**A**) Experimental design. Rats were injected chronically into the OFC with aCSF (vehicle) or NMDAR antagonists (AP5, TCN-201, or Ifenprodil) during the early (from day 1 to day 11) or late (from day 16 to day 26) post-acquisition periods and tested at day 30 following social interaction. (**B**) Early, but not late, post-encoding blockade of GluN2B subunits by intra-OFC infusions of ifenprodil impaired remote memory retrieval at day 30. The opposite pattern was observed when antagonizing GluN2A-NMDARs with TCN-201. Both early and late OFC infusions of the nonselective NMDAR antagonist AP5 impaired remote memory retrieval (early treatment effect: $F_{3,32} = 6.73$, $P < 0.05$; late treatment effect: $F_{3,37} = 4.09$, $P < 0.05$). *$P < 0.05$ versus aCSF (vehicle control), $n = 8$ to 13 rats per group. (**C**) Experimental design investigating relearning. Animals infused with aCSF (vehicle) or AP5 into the OFC during the early (from day 1 to day 11) or late (from day 16 to day 26) post-acquisition periods were submitted to a second interaction with a different flavor (cocoa) 1 week later (day 37). This novel memory for cocoa was assessed 30 days later to enable the establishment of remote memory in the OFC (day 67, choice between cocoa and cinnamon). (**D**) Groups previously injected with aCSF or AP5 during the early or the late post-acquisition periods exhibited a similar acquired preference for cocoa (group × delay: $F_{1,15} = 0.51$, $P > 0.48$, NS, $n = 8$ to 13 rats per group). The dotted line in (B) and (D) represents innate preference of FP control rats.

antagonist AP-5 impaired remote memory regardless of the targeted post-learning period (Fig. 3B and fig. S10, A and B). To rule out the possibility that these memory disruptions resulted from a nonspecific impairment in OFC function, we established that the same animals chronically infused with NMDAR antagonists could relearn and consolidate when tested 30 days after a second interaction with a demonstrator rat fed with a different flavor (Fig. 3, C and D, and fig. S10, C and D). Thus, these findings highlight a causal link between the functional rearrangement in GluN2B- and GluN2A-containing NMDARs at cortical synapses and memory consolidation and identify the GluN2B-GluN2A cortical switch as a crucial regulator of remote memory stabilization.

Operating features of the GluN2B-GluN2A cortical switch are compatible with the requirements of systems consolidation

What may drive such a consolidation-specific switch in the composition of synaptic NMDARs in the cortex as memories progressively mature over time? Contemporary models of memory consolidation posit that rewiring of cortical networks that support remote memory storage is under the post-learning guidance of the hippocampus (*2*, *3*, *5*, *29*). To test this, we trained rats in the STFP paradigm and temporarily silenced hippocampal activity during the two critical post-acquisition periods reported above to engage the hippocampus differently (Fig. 4A). As expected, remote memory impairment examined at day 30 occurred only when tempering with hippocampal function during the early (hippocampal-dependent), but not late (hippocampal-independent) period (fig. S11). Notably, this dissociation in memory performance was reflected in the GluN2A/GluN2B expression ratio in the OFC of a separate cohort of rats treated similarly but not tested at day 30 so as to avoid any confounding interference of memory retrieval on the rearrangement of cortical NMDAR subunits. Only early, but not late, hippocampal inactivation completely abolished the consolidation-induced increase of the GluN2A/GluN2B expression ratio normally observed remotely in the OFC of control rats with a functional hippocampus (Fig. 4B). Therefore, this result points to the crucial, but time-limited role, of the hippocampus in driving cortical wiring plasticity by acting, at least in part, on the balance in subunit composition of synaptic NMDARs of OFC neurons actively engaged in remote memory formation.

Because enduring memory representations are thought to be established incrementally in the cortex following highly congruent or repeated learning episodes (*3*, *30*), we next asked whether memory strength could act as a crucial determinant of the dynamics of hippocampal-cortical interactions, potentially leading, if increased

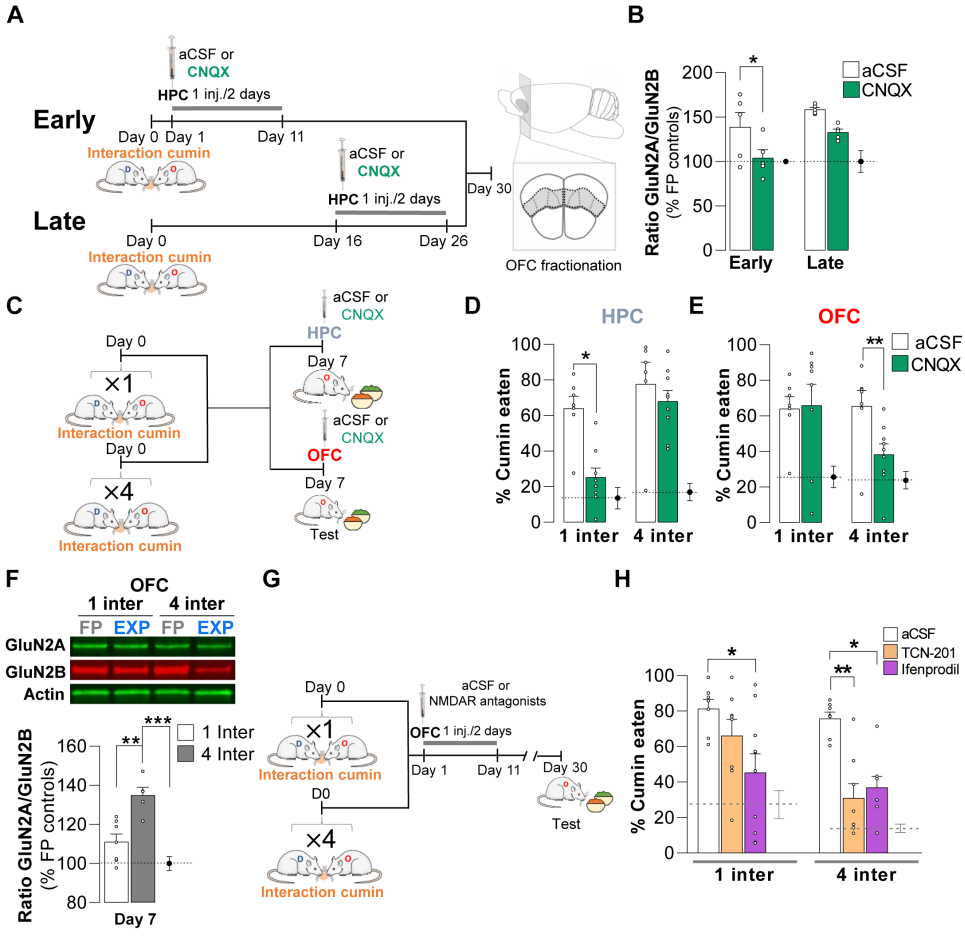

Fig. 4. Operating features of the consolidation-induced switch in the composition of cortical synaptic NMDARs. (**A** and **B**) Early, but not late, hippocampal inactivation with 6-cyano-7-nitroquinoxaline2,3-dione (CNQX) prevented the consolidation-induced rearrangement of cortical GluN2A and GluN2B subunit–containing NMDARs in the OFC ($F_{1,16} = 9.86$; $P < 0.001$); $^{*}P < 0.05$, $n = 5$ rats per group. (**C** to **E**), Memory strength (one versus four social interactions) modulated the post-acquisition kinetics of hippocampal and cortical involvement upon memory retrieval at day 7. CNQX-induced disruption of hippocampal activity after one interaction was no longer observed after four interactions (D, treatment × interaction number: $F_{2,37} = 4.519$; $P < 0.05$); $^{*}P < 0.05$, $n = 6$ to 9 rats per group). OFC dependency manifested after four, but not one, interactions (E, $F_{2,39} = 12.60$; $P < 0.0001$); $^{**}P < 0.01$, $n = 7$ to 9 rats per group). (**F**) Immunoblots (top) and corresponding quantitative analysis (bottom). An increase in the GluN2A-/GluN2B-NMDAR ratio was observed in the OFC at day 7 after four, but not one, interactions ($F_{2,13} = 16.51$; $P = 0.0003$); $^{**}P < 0.01$, $^{***}P < 0.001$, $n = 5$ to 7 rats per group. (**G** and **H**) Accordingly, blocking GluN2A-containing NMDARs with TCN-201 during the early post-encoding phase impaired remote memory retrieval at day 30 while being ineffective in the single interaction condition ($F_{1,26} = 17.22$; $P = 0.0003$); $^{*}P < 0.05$, $^{**}P < 0.01$, $n = 8$ rats per group; data from Fig. 3B are shown for comparison).

upon encoding, to an accelerated time course of embedding of cortical engrams compared to what is usually required for systems consolidation to be completed. To manipulate memory strength, we submitted independent groups of rats to an encoding session made of either one (regular training) or four (reinforced training) successive sessions of social interaction and tested their memory 7 days later (Fig. 4C). In these rats, we determined the respective involvement of the hippocampus and OFC upon retrieval by examining the effects of region-specific inactivation of neuronal activity. Concurring with previous results (*9*), silencing hippocampal functioning in the regular training protocol impaired memory retrieval, thereby highlighting hippocampal dependency (Fig. 4D and fig. S12, A and B). Accordingly, OFC inactivation was ineffective at this early time point (Fig. 4E and fig. S12, A and B). A different pattern of effects emerged with the reinforced procedure. As expected, stronger training produced robust associative olfactory memory in experimental controls (fig. S13). This time, however, retrieval was no longer dependent on the hippocampus (Fig. 4D and fig. S12, A and B) and engaged prematurely the OFC to ensure successful retrieval (Fig. 4E and fig. S12, A and B). Thus, increasing initial memory strength upon encoding (and presumably the amount of neuronal activation) enables memory traces to become more rapidly hippocampal independent and more quickly assimilated into cortical networks. Occurrence of the cortical switch in NMDAR subunit composition paralleled this faster rate of systems-memory consolidation in a dynamic manner, with an increased GluN2A/GluN2B ratio being observed as soon as day 7 (Fig. 4F) instead of days 15 and 30 in the OFC (see Fig. 1B for comparison). A temporal shift in the efficacy of intracortical NMDARs antagonists to impair remote memory retrieval further supported this accelerated cortical NMDAR synaptic reorganization. Interfering with GluN2A subunit–containing NMDARs after stronger encoding was indeed efficacious precociously during

the early post-training window (Fig. 4, G and H, and fig. S12, C and D), an effect only observable during the late post-training window in the regular encoding condition (Fig. 3, A and B). Together, these results identify the cortical switch in synaptic NMDAR composition as a highly responsive consolidation mechanism supporting memory formation and retrieval and potentially capable of coping with the experiential factors associated with a learning event.

Multiple engrams coexist in the cortex and influence consolidation of novel events depending on their maturation status and degree of similarity with oncoming information (*6*, *31*, *32*). Thus, nonoverlapping and overlapping populations of neurons are thought to be engaged in concert during engram formation while maintaining information specificity for a given engram (*32*, *33*). To determine whether the cortical switch in NMDAR subunit composition abides by this imperative rule, we submitted rats to two consecutive sessions of social interaction involving encoding of two different flavors (Fig. 5A). Microinfusions of NMDAR antagonists into the OFC were performed immediately before the second social interaction, thus authorizing adequate tagging of cortical cell assemblies coding for the first, but not the second, information (Fig. 5A). Early blockade of GluN2B subunit–containing NMDARs, but not of GluN2A subunit–containing NMDARs, in the OFC led to a robust impairment in remote memory retrieval probed at day 30 that was restricted to the second encoded flavor (Fig. 5B and fig. S14, A and B). This suggests that a specific pool of cortical neurons expressing GluN2B subunit–containing NMDARs at the PSD is allocated to a given memory trace at the time of encoding to support its cortical tagging and early post-training processing, thereby conferring to the cortical switch in NMDAR composition information specificity. Counterbalancing the order of presentation of the two flavors yielded similar results, thus ruling out possible confounding flavor- or salience-dependent effects (Fig. 5C and fig. S14, C and D). Likewise, nonspecific interference of NMDAR antagonists on encoding rather than consolidation processes was unlikely since pharmacologically challenged rats performed normally when tested for retrieval 4 days after interaction (Fig. 5, D and E, and fig. S14, E and F). Consistent with previous observations (*34*, *35*), AP5-induced blockade of NMDA receptors in the OFC did not alter remote memory retrieval

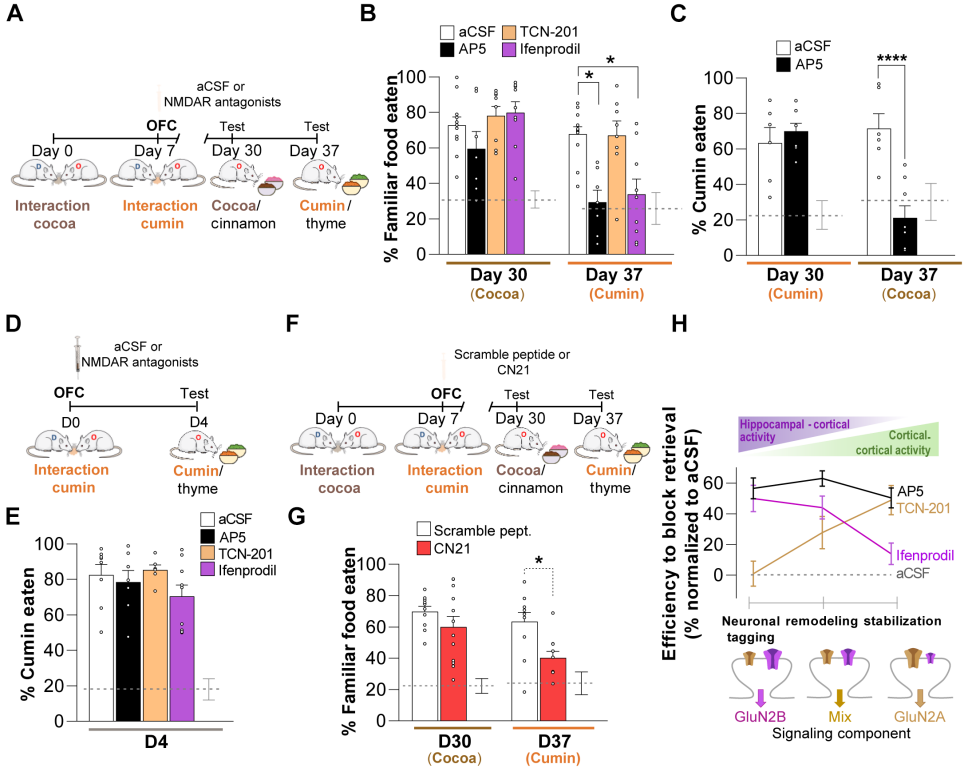

Fig. 5. Allocation of specific information to cortical synapses requires early recruitments of GluN2B subunit–containing NMDARs and CaMKII. (**A**) Experimental design investigating memory specificity. (**B**) Intra-OFC infusions of the GluN2B-NMDAR antagonist ifenprodil at the time of the second interaction (cumin) impaired remote memory for this second flavor while sparing remote memory for the first one (cocoa) (treatment × flavor pair: $F_{1,36} = 11.90$; $P = 0.0014$). The nonselective NMDAR antagonist AP5 exhibited a similar profile ($F_{1,32} = 17.31$; $P = 0.0002$). The GluN2A-NMDAR antagonist TCN-201 was ineffective regardless of the flavor pair (main treatment effect: $F_{1,34} = 0.28$; $P = 0.59$, NS). (**C**) Similar effects of AP5 infusions into the OFC were obtained when the two cumin/thyme and cocoa/cinnamon flavor pairs were counterbalanced (flavor × treatment: $F_{1,24} = 16.36$, $P < 0.001$). (**D**) Experimental design investigating encoding processes. (**E**) Intra-OFC infusions of AP5, TCN-201, and ifenprodil before social interaction did not impair performance of rats tested 4 days (D4) later (treatment effect: $F_{3,26} = 1.207$, $P > 0.33$, NS). (**F**) Experimental design investigating CaMKII contribution. (**G**) Intra-OFC infusions of the CaMKII inhibitor CN21 impaired formation of a newly encoded memory without destabilizing a previously encoded information undergoing consolidation ($F_{2,49} = 23.92$; $P < 0.0001$). (**H**) (Top) Efficacy of intra-OFC infusions of GluN2A- and GluN2B-NMDAR antagonists to impair remote memory retrieval at day 30 as a function of the specific phases of systems consolidation. Graph is based on findings from Fig. 3B and (B). (Bottom) Schematic of the GluN2A- and GluN2B-NMDAR redistributions at cortical synapses as enduring memories mature in the cortex. Size variation of NMDAR pictograms represents changes in the functional contribution of GluN2A- (in brown) and GluN2B-NMDARs (in pink). (B), (C), (E), and (G), $n = 6$ to 12 rats per group; $^*P < 0.05$, $^{****}P < 0.0001$.

(fig. S15, A and B). Thus, NMDA-dependent synaptic plasticity at encoding or during the post-learning period appears essential for guiding memory consolidation but not for retrieval. Mechanistically, within the PSD, GluN2B subunit–containing NMDARs are major binding and functional partners of the Ca^{2+}/calmodulin (CaM)–dependent protein kinase II (CaMKII), which is thought to serve as a molecular basis of engram formation (*36*). Accordingly, infusing the CaMKII inhibitor CN21 into the OFC immediately before memory encoding impaired remote memory retrieval at day 30 in an information-specific manner (Fig. 5, F and G, and fig. S16), highlighting the essential contribution of CaMKII-GluN2B protein complexes to synaptic signaling elicited upon early tagging of cortical networks.

Redistribution of synaptic GluN2A- and GluN2B-containing NMDARs in the cortex controls the fate of remote memory

As summarized in Fig. 5H, encoding-induced changes in the composition of NMDARs at cortical synapses time-locked to specific phases (cortical tagging, remodeling, and stabilization) of the consolidation process to promote the formation of enduring memories. We next wondered how these reorganizations in synaptic NMDARs take place. Although perisynaptic endocytosis and exocytosis processes control the surface pool of receptors (*37*), lateral diffusion of NMDARs allowing receptors to enter and exit synapses has emerged as a necessary step for the regulation of receptor composition of the PSD during activity-dependent synaptic adaptations (*17*, *20*, *38*). This prompted us to explore whether interfering with the surface diffusion–based redistribution of GluN2B and GluN2A subunit–containing NMDARs during the multiphasic process of systems-level consolidation could prevent remote memory formation. To selectively manipulate the surface redistribution of GluN2B-NMDARs, we implemented an antibody-based cross-linking (x-link) strategy previously designed to immobilize receptors without harming their channel properties (*20*). Single-particle tracking on cultured cortical neurons revealed that application of immunoglobulins targeting the N-terminal domain of GluN2B subunits selectively limited surface redistributions of GluN2B-containing NMDARs (fig. S17, A to C) as attested by a leftward shift of the mean square displacement (MSD) curve (fig. S17C) and a marked increase of the immobile fraction of these receptors (fig. S17, D to G). We then transposed this approach to STFP-tested rats infused with GluN2B-specific antibodies into the OFC during the early, GluN2B-NMDAR–dependent, remodeling phase of memory consolidation (Fig. 6A). Critically, preventing redistributions of GluN2B-containing NMDARs after encoding from day 1 to day 25 selectively impaired remote memory retrieval at day 30, indicating dysfunctional remote memory formation (Fig. 6B and fig. S18). The consolidation-induced increase in the GluN2A/GluN2B ratio normally occurring at OFC synapses of remotely tested rats injected with control (ineffective) antibodies was abolished in rats treated with intra-OFC infusions of GluN2B-specific

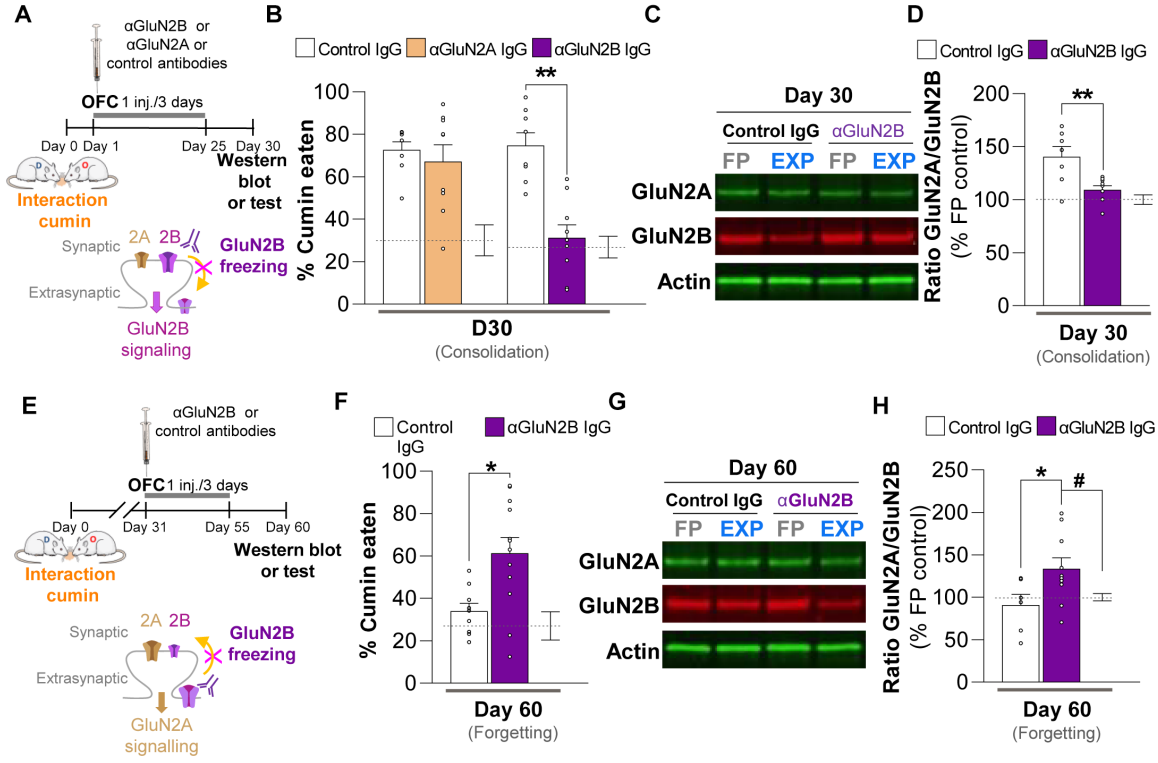

Fig. 6. Modulating redistributions of GluN2B-containing NMDAR at cortical synapses determines the fate of remote memory. (**A** to **D**) Intra-OFC infusion of an anti-GluN2B, but not of an anti-GluN2A, antibody during the early post-encoding period (A) impaired remote memory retrieval assessed 30 days later (B, group × treatment interaction: $F_{1,38} = 16.10$; $P = 0.0003$) and abolished the increase in GluN2A-/GluN2B-NMDAR ratio observed in the OFC of control rats (D, $F_{2,19} = 10.45$; $P = 0.0009$); $^{*}P < 0.05$, $^{**}P < 0.01$, $n = 8$ to 9 rats per group. (**E** to **H**) Intra-OFC delivery of the anti-GluN2B antibody during the late post-encoding period (E) prevented forgetting (F, $F_{2,32} = 7.67$; $P = 0.0019$) and the decrease of the GluN2A-/GluN2B-NMDAR ratio in the OFC (H, $F_{2,18} = 5.88$; $P = 0.0109$) normally seen in control rats at day 60. $^{*}P < 0.05$, $^{\#}P < 0.05$, $n = 10$ to 14 rats per group. Immunoblots in (C) and (G) served for quantification of respective GluN2A-/GluN2B-NMDAR ratios.

antibodies, attesting to the efficacy of the in vivo x-link approach to block GluN2B-NMDA redistribution (Fig. 6, C and D, and fig. S19, A and B). Preventing redistributions of GluN2A-containing NMDARs using a similar x-link strategy (fig. S20) had no impact on remote memory retrieval (Fig. 6B and fig. S18), suggesting that GluN2B-NMDAR diffusion-based redistributions primarily contribute to the changes in the GluN2A-/GluN2B-NMDAR ratio at OFC synapses supporting memory consolidation. This lack of effect also renders unlikely that the observed GluN2B antibody–induced memory disruption was due to a nonspecific confound of antibody injections into the OFC or an effect of antibodies on NMDAR channel properties. Thus, GluN2B-NMDARs at cortical synapses constitute a crucial determinant of remote memory formation.

Given that forgetting observed at day 60 was associated with a progressive increased synaptic expression of GluN2B subunit–containing NMDARs (Fig. 1B and fig. S3E), we next reasoned that redistribution of GluN2B subunit–containing NMDAR could potentially contribute to memory degradation over time. We thus predicted that immobilizing GluN2B-containing NMDARs during the late stabilization phase of memory consolidation should prolong enduring memories. To test this, we delayed the intra-OFC delivery of GluN2B-specific antibody to target this specific post-training period (Fig. 6E). Notably, infusing GluN2B-specific antibodies from day 31 to day 55 after encoding maintained the GluN2A-/GluN2B-NMDAR ratio at OFC synapses to previous post-consolidation levels and prevented memory decay normally observed in control rats at day 60 (Fig. 6, F to H, and fig. S21). Thus, preventing the reincorporation of GluN2B-NMDARs at cortical synapses so as to preserve the contribution of GluN2A-NMDARs may have strengthened synaptic stability, making cortically embedded memory engrams less prone to deterioration and potentially more resistant to the passage of time.

DISCUSSION

How encoded memories are selected for subsequent consolidation and acquire long-term stability is still a matter of debate (*4*, *39*). Our findings identify the experience-dependent nanoscale rearrangement of cortical NMDAR subtypes (or "consolidation switch") as an essential synaptic mechanism whose operating features enable control on the formation and dynamics of enduring memories in the cortex.

NMDARs operate within a synaptic territory composed of multiple signaling proteins that can fine-tune their functional roles (*40*). Among these, CaMKII, which binds to GluN2B subunits (*41*–*43*), has been identified as a critical molecular organizer of synaptic plasticity during the course of memory consolidation (*44*–*46*). How then may cortical GluN2B-containing NMDARs at cortical synapses elicit experience-dependent plasticity? Insights can be gained from ex vivo studies showing that GluN2B-NMDAR surface redistribution favors the activity-dependent recruitment of CaMKII to the PSD (*20*). We suggest that these GluN2B-CaMKII complexes could serve as a structural seed for the recruitment of other proteins, including AMPA receptors, leading to growth of specific potentiated synapses (*36*, *40*, *47*, *48*) and continuous adjustment of their plasticity threshold (*49*). Such GluN2B-NMDAR redistribution–based form of tuning appears as a necessary step to ensure the creation of a cortical engram cell network bearing either persistence via stability in its synaptic connectivity or malleability to accommodate novel incoming information, update existing consolidated events via synaptic turnover, or initiate forgetting as predicted by computational models (*50*). While driven by experience-specific neuronal activity initiated upon encoding, the rearrangement in GluN2A and GluN2B subunit–containing NMDARs at cortical synapses we report here may likely contribute to homeostatic plasticity, which has been suggested to lead to the formation of remote memories by stabilizing engram network dynamics (*51*). Within this framework, the consolidation switch in NMDAR subunits could act as a "homeostatic gatekeeper" within network-wide engram cells, controlling the synaptic plasticity threshold to either stabilize engram synapses or enable their reallocation. Hence, rather than driving memory consolidation per se, the consolidation switch could thus optimize or orientate NMDAR plasticity within neuronal networks actively engaged in systems consolidation.

Our observations have implications for the neurobiology of learning and memory. First, post-encoding changes in the composition of synaptic NMDARs that we found to be associated to specific phases of the systems-level consolidation process concur with the previously envisioned bidirectional malleability of the synapse—a property that makes it a highly responsive element capable of tuning neuronal connectivity either positively or negatively (*52*). This property echoes the concept of memory malleability, which has been intensively debated in the context of psychological studies of human memory. Far from being a reproductive entity, the consensus that has emerged from these investigations is that memory appears largely reconstructive, potentially making recollections of past events more adaptive to the changing world (*10*, *53*). Thus, contrasting with established views, memory consolidation should be seen as a never-ending process of reorganization rather than a one-time process enabling memory to be acquired inflexibly over extended period of time (*11*). Corticalized remote memories can reorganize over time, undergoing updating (*54*) or even transformation (*55*). The operating features of the consolidation switch we have uncovered make it a relevant cortical mechanism capable of coping with these requirements. Such a mechanism provides a neurobiological basis for a reappraisal of the long-held defining features of enduring cortical engrams reflected in current theories of systems consolidation. Rather than immutable, these cortical engrams remain malleable across time. Our findings suggest that, in the adult learning cortex, GluN2A-NMDARs preferentially act as a "synapse stabilizer," while GluN2B-NMDARs make the synapse more permissive to activity-dependent changes in synaptic strength. Consolidation-induced changes in NMDAR function occurred independently of response amplitude (Fig. 2B and fig. S9, E and F), indicating that it is the relative composition in cortical NMDAR subunits at the synapse that determines the fate of remote memory. Although differentially expressed during the multiphasic process of systems consolidation, both GluN2A- and GluN2B-NMDARs remained present at cortical synapses of engram cells. In this way, the intrinsic plastic capacity within engram cell networks is preserved, albeit with a tunable threshold, thereby conferring to cortical engrams a persisting and highly responsive form of malleability. This property has practical implications. By allowing multiple cortical engrams to dynamically interact and be flexibly processed, the consolidation switch in the synaptic organization of NMDAR subunits may adapt the quality of memory recall by generating either vivid (richly detailed) or more schematic (gist-like) memories as a function of the retrieval circumstances (*56*), correct previously consolidated memories, or even lead to their distortion by incorporating misinformation (*53*).

Second, that the fate (i.e., persistence or erasure) of a memory can be manipulated during the course of its cortical assimilation by directly acting upon NMDAR redistributions at cortical synapses points to the potential of the cortex to function as a highly responsive and flexible consolidation system—contrasting with the traditional view of it being a rigid and slow incremental learner exclusively under the teaching of hippocampal inputs (*57*). Experiential factors can accelerate the rate of hippocampal-cortical interactions during systems-level consolidation. We tested here the impact of memory strength upon encoding, but previous accounts have shown that cortical consolidation can also occur rapidly when prior knowledge (i.e., a mental schema) is already embedded cortically (*58*). The highly dynamic consolidation switch, as reflected by the intrinsic capability of NMDAR subunits to diffuse in and out synapses at high speed (*17*), has the adaptability features to support such a faster consolidation mode. For instance, this synaptic mechanism could help alleviate the processing load imposed on the hippocampus, and perhaps even bypass the hippocampal engagement, to ensure updating of cortical mental schemas with minimal catastrophic interferences (*54*).

Third, the consolidation switch we have identified offers an effective synaptic mechanism for managing active forgetting of cortically embedded memories. By rapidly tilting the balance toward either GluN2A- (engram stabilization) or GluN2B-NMDARs (engram degradation) at specific cortical synapses of a given memory engram circuit, NMDAR surface diffusion may provide the brain with an inherent system capable of dynamically arbitrating, within the same synaptic locus, the competition between persistence, erosion, or recycling of cortical engrams. Complementary to previously described mechanisms of forgetting, this essential tuning system may accommodate a form of "intrinsic-based forgetting," which relies on an array of signaling proteins controlling the synaptic connectivity between engram cells (*59*). Whether NMDAR redistribution–based forgetting alters the integrity of memory engrams resulting in their irreversible erasure, or only disrupts retrieval of preserved enduring engrams, remains to be elucidated. Alternatively, this tuning system may contribute to the partial weakening of cortical engrams, including unused ones, such that a stored engram remains available for retrieval but can only be accessed efficiently in retrieval situations satisfying encoding specificity or permitting high engram reactivation (*60*).

Cortical engrams are thought to coexist in silent (inaccessible) and active (retrievable) forms (*61*) and may differentially engage the hippocampus for their expression (*11*). Within this framework, the consolidation switch in the synaptic organization of cortical NMDARs may contribute actively to this delicate engram dynamics by tuning synaptic efficacy between engram cells, thereby determining which cells are recruited to an engram upon encoding (neuronal allocation) and which engrams achieve stability (memory persistence), are reallocated (memory updating and/or transformation) or undergo dematuration (retrieval failure or memory erasure). We dedicated our attention to the OFC due to its privileged role as a permanent repository of enduring associative olfactory memories (*9*, *24*). Formation of these memories, however, requires a time-dependent involvement of the hippocampus for their cortical embedding, raising the possibility that encoding-induced changes in the synaptic organization of GluN2A- and GluN2B-NMDARs can also occur in this brain region, albeit with a different timescale. The finding of a selective involvement of hippocampal CA1 NMDAR surface trafficking in the temporal component of associative memory supports this possibility (*18*). Because hippocampal inputs are temporally limited (*9*) (see also fig. S11), a switch in the subunit composition of hippocampal NMDARs would have to take place precociously during the early phase of the consolidation process. Functionally, we can speculate that such synaptic changes, if occurring, could contribute to the creation of a hippocampal index (or "pointer" to cortical locations), which is thought to serve as a coincidence regenerator for promoting the formation of relevant set of engram cells in the cortex (*62*, *63*). Thus, hippocampal and cortical NMDAR trafficking could potentially act in concert to promote early and late engram consolidation within hippocampal-cortical networks.

Implementing dedicated tools to investigate the contribution of NMDAR redistributions selectively is challenging. The x-link strategy carried out here allowed us to manipulate NMDAR surface redistribution without interfering with NMDAR channel properties (*20*). However, besides preventing surface diffusion–based NMDAR redistributions, antibody-elicited receptor aggregation in vivo for a prolonged period of time may lead to receptor internalization (*64*). Thus, we cannot exclude that part of the consolidation-occluding action of antibodies involves endocytosis of GluN2B subunit–containing NMDARs, which could result in a decreased incorporation of GluN2B-NMDARs at cortical synapses and a reduction of overall NMDAR-mediated synaptic currents. However, the parallel observation of GluN2A-NMDAR–targeting antibodies having no impact on memory performance—although they efficiently prevented redistributions and potentially caused receptor internalization as well—indicates that antibody-elicited consolidation impairments more likely result from preventing NMDAR surface redistribution. Together, these observations further support a causal link between activity-dependent synaptic rearrangements of NMDARs and memory consolidation.

The operating features of the consolidation switch are compatible with the various experiential factors associated with a learning event and support the challenging concept that a consolidated memory, rather than being fixed, remains a malleable entity with the ability of constantly reorganizing over a lifetime. Neuronal reactivations during post-encoding periods of quiet restfulness or sleep are considered a core process for driving synaptic reorganization and successful consolidation of episodic memories (*65*). Although further investigations are required, we speculate that the lateral diffusion of NMDARs at cortical synapses may also constitute an important partner during these specific offline periods to coordinate the reorganization of cortical engrams.

MATERIALS AND METHODS

Animals

Male Sprague-Dawley rats (RjHan:SD, RRID:RGD_38676310, Janvier Breeding Center, Le Genest Saint Isle, France) weighing 225 to 250 g at the beginning of experiments were used throughout. All rats were housed individually during behavioral experiments in polycarbonate standard rat cages and maintained on a 12:12-hour light-dark cycle [as previously described (*27*)]. Food, water, and various objects serving as cage enrichment were freely available except during behavioral training when rats were food-restricted to 90% of their free-feeding body weight. Behavioral experiments were conducted during the light phase of the cycle. All experimental procedures complied with official European Guidelines for the care and

use of laboratory animals (directive 2010/63/UE). They were approved by the ethical committee of the University of Bordeaux and validated by the French Ministry of Higher Education, Research, and Innovation (authorization number: A50120159). The ARRIVE guidelines (Animal Research: Reporting of In Vivo Experiments) were applied across experiments (*66*).

The STFP task

Procedure

The STFP task used to assess associative olfactory memory was performed as previously described in detail by Bessières *et al.* (*27*). Rats underwent the classical three-step procedure. Briefly, demonstrator rats were food-restricted and then habituated to eating either plain or cumin powdered chow for 3 days (30-min session). Observer rats were also shaped for 3 days to consume plain powdered chow from two cups placed in their home cage.

For the interaction session, the demonstrator rat was first allowed 30-min access to one cup filled with plain, cumin (0.5%, i.e. 0.5 g of cumin mixed with 99.5 g of plain powdered chow) or cocoa (2%) powdered chow (water was removed from the cage) and was then moved to the observer's cage fitted with a stainless steel wire mesh divider. Food-restricted observer rats were kept in the opposite side of their cage for a 20-min interaction period at the end of which the divider was removed, allowing the two rats to interact freely for another 10 min. At the end of this 30-min interaction period, the demonstrator rat was removed from the cage. Observer and demonstrator rats were always unfamiliar with each other.

At retrieval testing, after a selected retention interval (1, 15, 30, or 60 days depending on the experiment), each food-restricted observer rat was presented in its home cage with a choice of two cups containing a novel food (0.75% thyme or 1% cinnamon powdered chow) and the familiar food that the demonstrator rat had consumed before interacting with the observer rat (0.5% cumin or 2% cocoa powdered chow). The position of the familiar food (left or right) in the cage was counterbalanced across the different groups. After 20 min, the cups were removed and weighed, and olfactory-associative memory performance for a given flavor pair (cumin/thyme or cocoa/cinnamon) was expressed as percentage of familiar food eaten (% cumin or % cocoa) using the following formula: amount of familiar food eaten / amount of total food) × 100. The rats were expected to consume a total of at least 2 g of scented food to generate a reliable index of memory performance. This index was used as an exclusion criterion. We systematically verified that the observer rat sampled both cups and left a nose mark on the surface of the nonpreferred cup. Although observer rats rarely eat exclusively from one cup, a completely untouched cup was an additional criterion to exclude the animal from analysis. Experiments were replicated at least twice using separate cohorts of animals.

Flavor concentrations within each food pair (cumin/thyme and cocoa/cinnamon) were chosen in pilot experiments to induce an innate preference for one given flavor (i.e., thyme and cinnamon, respectively). Use of these two biased flavored pairs enabled to decrease the chance level at test and thus to optimize the possibility of detecting changes in memory performance across our various treatments (*27*). At the concentrations used for the cumin/thyme flavor pair for example, we found that rats naturally prefer thyme over cumin. However, interaction with a demonstrator that has eaten cumin powdered chow could reverse this innate preference so that observers chose cumin over thyme (up to 80% of the total food eaten, chance level of ~20%).

STFP main features

By interacting with a demonstrator rat that has recently eaten a novel flavored food (e.g., cumin), note that the observer rat forms an association between this food odor and some constituents of the demonstrator's breath [i.e., carbon disulfide (*26*, *27*)]. Subsequently, when submitted with a choice between cumin and a new flavored food, the observer rat expresses a memory for this association by preferentially choosing the same food odor that was present in the demonstrator's breath because it is considered without danger and therefore safe to eat. Accordingly, this paradigm taxes associative olfactory memory and does exhibit some of the key features of declarative memory that is, information about potential food sources can be encoded rapidly and expressed flexibly in a test situation different from the circumstances encountered during initial learning (*67*). The STFP paradigm has been shown to be dependent on hippocampal function (*5*, *9*, *68*) and is particularly well-suited for the investigation of remote memory formation because a single training session produces robust and long-lasting memories (main Fig. 1A).

The fact that encoding of associative olfactory memory occurs within only one brief training session provided rigorous control over the time course of hippocampal-cortical interactions underlying systems-level memory consolidation and avoided repeated (over days) initial training sessions as is often the case in complex spatial tasks. In addition, we were careful in testing the observer rat in its home cage kept in the same location of the animal facility, thereby reinforcing the nonspatial component of the STFP task. This enabled us to better isolate the functional implication of the hippocampus in systems-level consolidation by minimizing hippocampal-dependent processing of spatial information.

Control groups

To ensure that the different drug treatments used throughout experiments did not change the innate preference of the animals for thyme and cumin (or cocoa and cinnamon) and to establish chance levels experimentally for the flavored pair, additional FP control groups were added to each experiment. These groups were treated similarly as experimental animals and received identical drug treatments. In all our pharmacological experiments, note that we did not observe any significant difference in the percentage of familiar food eaten between FP groups receiving vehicle or a given drug. Therefore, their performance was pooled to generate the experimental chance level represented on graphs by a dotted line and its associated standard error mean.

Experimental designs

Assessing memory performance in the STFP task relies exclusively on the amount of food eaten by the animals. To rule out the possibility that targeted intracerebral drug treatments interfered with motivational processes, our experiments were designed to control as much as possible for this potential confounding factor by adding the relevant control groups for each targeted brain region (i.e., vehicle-injected groups, use of two or more retention delays for a given targeted brain region enabling to show a delay-dependent pharmacological effect on memory performance in the absence of any treatment effect on total food consumption). Experimental designs of most experiments are depicted in a dedicated panel of each main or supplementary figure.

Tissue preparation, subcellular fractionation, and Western blot analysis

Tissue preparation

To rule out the possibility that retrieval processes, in addition to memory consolidation per se, contributed to the observed changes in the subunit composition of cortical NMDARs, experimental and FP control rats underwent the STFP procedure without being subsequently tested for memory retrieval. Observer rats were terminally anesthetized with a mixture of Exagon (pentobarbital, 300 mg/kg; Axience, Pantin, France) and Lurocaine (20 mg/kg; Vetoquinol, Lure, France) injected intraperitoneally and decapitated after a selected retention interval (1, 15, 30, or 60 days, depending on the experiment).

Subcellular fractionation

As previously described (*69*), OFC and parietal cortex were dissected on ice in cold phosphate-buffered saline (PBS) and homogenized in 200 µl of 0.32 M sucrose buffer [10 mM sucrose and 10 mM Hepes (pH 7.4)] containing a protease inhibitor cocktail (Sigma-Aldrich, L'lsle D'Abeau Chesnes, France). Samples were centrifuged (1000*g* for 10 min at 4°C) to yield the nuclear-enriched pellet and the S1 fraction. The S1 fraction was then centrifuged (12,000*g* for 20 min at 4°C) to obtain supernatant (S2, microsomes and cytosol) and pellet (P2, crude synaptosomal membranes) fractions. The P2 synaptosomal pellet was resuspended in 100 µl 4 mM Hepes buffer [4 mM Hepes and 1 mM EDTA (pH7.4)] and again centrifuged (12,000*g* for 20 min at 4°C). Resuspension and centrifugation were repeated. The resulting pellet was resuspended with buffer A [20 mM Hepes, 100 mM NaCl, and 0.5% Triton X-100, (pH 7.2)] and rotated slowly (15 min, 4°C) followed by centrifugation (12,000*g* for 20 min at 4°C). The supernatant, (Triton X-100–soluble fraction) containing non-PSD membranes was retained. The pellet was resuspended in 120 µl of buffer B [20 mM Hepes, 0.15 mM NaCl, 1% Triton X-100, 1% deoxycholic acid, 1% SDS, and 1 mM dithiothreitol (pH 7.5)] followed by gentle rotating (1 hour, 4°C) and centrifugation (10,000*g* for 15 min at 4°C). The pellet was discarded and the supernatant (Triton X-100 insoluble, i.e., PSD fraction) retained. PSD samples were stored at −80°C until use.

Western blots

Electrophoresis was performed on precast 4 to 15% polyacrylamide tris-glycine gels (Bio-Rad, Marnes-la-Coquette, France). Blots were treated as previously described (*70*). Protein levels were normalized to 20 µg of protein per sample and resuspended with 4× Laemmli sample buffer (Bio-Rad, Marnes-la-Coquette, France) before boiling (5 min at 95°C). Then, proteins were transferred onto a polyvinylidene difluoride (PVDF) membrane (Bio-Rad, Marnes-la-Coquette, France). Membranes were blocked with tris-Tween–buffered solution [(TTBS 10 mM, tris, 200 mM, NaCl 0.05%, Tween 20 (pH 7.4)] containing 5% nonfat dry milk for 1 hour at room temperature. The blots were then incubated overnight at 4°C with a mouse anti-GluN2B antibody (RRID: AB_827426; catalog number: MAB5778; 1:1000; Millipore, Molsheim, France) and a rabbit anti-GluN2A antibody (RRID:AB_1163481; catalog number: 04-901; 1:1000; Millipore, Molsheim, France). Primary antibodies were probed with an IRDye 800CW goat anti-rabbit immunoglobulin G (IgG) (RRID: AB_2651127; catalog number: 925-32211; dilution 1:5000; Li-Cor Biosciences, Bad Homburg, Germany) together with an IRDye 680RD goat-anti mouse IgG (RRID: AB_10956588; catalog number: 926-68070; dilution 1:5000; Li-Cor Biosciences, Bad Homburg, Germany) during 1 hour of incubation at room temperature. After three washes with TTBS and one with PBS, each membrane was scanned using the automated infrared imaging system Odyssey (Li-Cor Biosciences, Bad Homburg, Germany) according to the manufacturer's instructions. Blots were thereafter incubated in a stripping buffer before being reprobed with an anti-actin antibody (RRID:AB_476693; catalog number: A2066; 1/2000; Sigma-Aldrich, L'lsle D'Abeau Chesnes, France) and revealed as described above. Detection of actin protein on the same membrane was used as a loading control.

Electrophysiology

Rats received an intra-OFC stereotaxic injection of a viral construct (0.8 µl, 5.84×10^7) infectious particles per milliliter; Fig. 2A) allowing the constitutive expression of the RFP and the activity-dependent expression of a fluorescent reporter of neural plasticity based on an E-SARE within the *Arc* promoter to track neurons that are recruited upon memory retrieval (*28*). The plasmid was provided by H. Bito (Department of Neurochemistry, Graduate School of Medicine, The University of Tokyo, Tokyo, Japan), and the viral particles were produced at our vectorology platform Vect'UB (CNRS UMS 3427, INSERM US05, Univ. Bordeaux, Bordeaux, France). Following a recovery period of 14 days, intracortically injected rats were submitted to STFP training. They were tested for memory retrieval (choice between cumin and thyme flavored food cups) either 1 or 30 days following social interaction (encoding phase) and deeply anesthetized (intraperitoneal injection of a mixture of Exagon (pentobarbital, 300 mg/kg) and Lurocaine, (20 mg/kg) 90 min after completion of retention testing. The animals were euthanized by decapitation, and their brains were collected to perform electrophysiological recordings from OFC neurons engaged in memory testing in acute brain slice preparations (*20*). Acute parasagittal brain slices (350 mm thick) were prepared in a dissection solution containing (in mM): 250 sucrose, 2 KCl, 7 $MgCl_2$, 0.5 $CaCl_2$, 1.15 NaH_2PO_4, 11 glucose, and 26 $NaHCO_3$ and equilibrated with 95% O_2 and 5% CO_2. Slices were then incubated at 33°C for 30 min and subsequently stored at room temperature in an oxygenated artificial cerebrospinal fluid (aCSF, gassed with 95% O_2 and 5% CO_2) containing (in mM): 126 NaCl, 3.5 KCl, 2 $CaCl_2$, 1.3 $MgCl_2$, 1.2 NaH_2PO_4, 25 $NaHCO_3$, and 12.1 glucose (pH 7.35).

Whole-cell voltage-clamp recordings from naive infected (expressing RFP only) or behaviorally activated (expressing RFP and GFP) OFC neurons were made at 33°C under infrared differential interference contrast imaging. Spontaneous NMDAR-mediated EPSCs (sEPSCs) were recorded at +40 mV in the presence of the γ-aminobutyric acid type A ($GABA_A$) receptor antagonist SR 95531 hydrochloride (10 µM), the $GABA_B$ receptor antagonist CGP 55845 hydrochloride (5 µM), and the AMPA receptor antagonist NBQX (10 µM). After a baseline recording period of 10 min, Ro 25-6981 (2 µM) was further added to selectively inhibit GluN2B-containing NMDAR and evaluate the relative contributions of GluN2A- and GluN2B-containing receptors to NMDAR-mediated sEPSCs. Recording electrodes (4 to 5 megohm) were filled with a solution containing (in mM): 125 cesium methane sulfonate, 4 NaCl, 2 $MgCl_2$, 10 Hepes, 10 EGTA, 5 phosphocreatine, 2 MgATP, 0.33 Na_3GTP, and 5 QX-314 (adjusted to pH 7.2 with CsOH). All drugs and reagents were purchased from Tocris Bioscience (Bristol, UK) or Sigma-Aldrich (Sigma-Aldrich, L'lsle D'Abeau Chesnes, France).

Data were recorded using a Multiclamp 700B amplifier and a Digidata 1550B interface controlled by Clampex 10.7 (Molecular Devices, Berkshire, UK). Signals were sampled at 20 kHz and low-pass

filtered at 2 kHz, respectively. NMDAR-mediated sEPSC detection and analysis were performed using an in-house software (Detection Mini, developed by M. Goillandeau). Access resistance and leak currents were monitored continuously, and experiments were discarded if these parameters changed by more than 20% during recording (*48*).

Stereotaxic surgery

Under deep general anesthesia induced by a mixture of ketamine (100 mg/kg, Virbac, Carros, France) and xylazine (12 mg/kg, Elanco, Sévres, France) injected intraperitoneally and complemented by a subcutaneous administration of buprenorphin (Buprecare, 0.05 mg/kg, Centravet, Dinan, France), the rats were implanted bilaterally with stainless steel guide cannulae using the following stereotaxic coordinates (*71*): (i) hippocampus (HPC): anteroposterior (AP) relative to bregma, −3.8 mm; lateral (L) to midline, ±2 mm; ventral (V) from the skull surface, −2 mm. (ii) OFC: AP, +4.2 mm; L, ±2 mm; V, −2.7 mm. The rats were allowed a minimum of 2 weeks to recover before being submitted to memory testing.

Intracerebral infusion procedure

Various drugs were infused intracerebrally using an injection cannula projecting 1.5 mm beyond the tip of the guide cannula. For hippocampus, 1 μl was injected at a rate of 0.8 μl/min; for OFC, 0.8 μl was injected at a rate of 0.6 μl/min. Anatomical specificity is a critical issue when pharmacologically modulating neuronal activity within brain regions. Therefore, only animals with cannula tips correctly located within targeted structures were included in the study. To minimize any carryover effects of drugs administered during the consolidation period on memory retrieval, intracerebral injections were stopped 3 days before retrieval testing.

Drugs

D-2-amino-5-phosphonovalerate (AP5) (catalog number: 0106/1; Tocris, Bristol, UK) was prepared as a stock solution of 5 μg/μl in aCSF (catalog number: 3525; Tocris, Bristol, UK) and aliquoted before being stored at −20°C. The aliquots were later thawed, and 0.8 μl (4 μg) was bilaterally injected into the OFC (Figs. 3, B and D, 5, B, C, and E, and figs. S10, S14, and S15).

Ifenprodil (catalog number: 0545; Tocris, Bristol, UK) was prepared as a stock solution of 37.5 nmol/μl in aCSF and aliquoted before being stored at −20°C. The aliquots were later thawed, and 0.8 μl (30 nmol) was bilaterally injected into the OFC (Figs. 3B, 4H, and 5, B and E, and figs. S10B, S12D, S14B, and S14F).

3-Chloro-4-fluoro-*N*-[4-[[2-(phenylcarbonyl)hydrazino]carbonyl]benzyl]benzenesulfonamide or TCN-201 (catalog number: 4154, Tocris, Bristol, UK) was prepared as a stock solution of 1.25 nmol in aCSF and aliquoted before being stored at −20°C. The aliquots were later thawed, and 0.8 μl (1 nmol) was bilaterally injected into the OFC (Fig. 3B, 4H, and 5, B and E, and fig. S10B, S12D, S14B, and S14F).

TAT-CN21 or TAT-control was provided by Dr. Bayer (Department of Pharmacology, University of Colorado, Denver, USA) and prepared as a stock solution at 20 nmol in aCSF and aliquoted before being stored at −20°C. The aliquots were later thawed, and 0.8 μl (16 nmol) was bilaterally injected into the OFC (Fig. 5G and fig. S16).

The AMPA receptor antagonist 6-cyano-7-nitroquinoxaline2,3-dione was prepared as a stock solution of 3 mM in aCSF and aliquoted before being stored at −20°C. The aliquots were later thawed, and 1 μl or 0.8 μl was bilaterally injected into the HPC (3 nmol) (Fig. 4, B and D, and figs. S11 and S12B) or the OFC (2.4 nmol), respectively (Fig. 4E and figs. S2 and S12B).

The selective sodium channel blocker tetrodotoxin (catalog number: T8024, Sigma-Aldrich, L'lsle D'Abeau Chesnes, France) was prepared as a stock solution of 12.5 ng/μl in aCSF and aliquoted before being stored at −20°C. The aliquots were later thawed, and 1 μl was bilaterally injected into the HPC (fig. S2, B and D).

Immunocytochemistry and brain imaging

Observer rats were terminally anesthetized with an intraperitoneal mixture of Exagon (pentobarbital 300 mg/kg) and Lurocaine (20 mg/kg) and perfused transcardially with 0.9% saline and 4% paraformaldehyde (catalog number: P-6148, Sigma-Aldrich, L'lsle-d'Abeau Chesnes, France) 90 min after completion of retention testing. The brains were removed and prepared for immunocytochemistry on free-floating sections as previously described (*9*). Fifty-μm-thick sections, generated with a vibratome, were washed in phosphate buffer (PB) 0.1 M and incubated in blocking solution [0.1% bovine serum albumin (BSA), 2% goat serum, and 0.2% Triton X-100 in PB 0.1 M] for 2 hours. The sections were then incubated in primary antibody overnight at 4°C in blocking buffer. The following primary antibodies were used: rabbit polyclonal anti–*c-fos* (RRID: AB_2247211; catalog number: mAb #2250; 1:500; Cell Signaling Technology, Danvers, USA) and rabbit polyclonal anti-*arc* (RRID: AB_887694; catalog number: 156003; 1:1000; Synaptic System, Goettingen, Germany). After three washes in PB 0.1 M, slices were incubated with a Cy3 goat anti-rabbit secondary antibody (catalog number: 111-165-144; dilution; Jackson ImmunoResearch, Ely, UK) in blocking buffer for 2 hours at room temperature and washed three times before mounting on glass slides and covered with Fluoromount-G mounting medium (Southern Biotech, Birmingham, USA).

Fluorescent images were acquired with an Olympus microscope with a 20× objective. Quantitative analyses of positively labeled nuclei were performed using ImageJ. Structures were anatomically defined according to the Paxinos and Watson atlas (*71*). Immunoreactive neurons were counted bilaterally by an experimenter blind to the experimental conditions. Total Fos^+ or Arc^+ cells in a given structure were counted and averaged across rats to generate the final mean of each group.

Single-particle tracking

Cultures of cortical neurons were prepared from E18 embryo Sprague-Dawley rats. Briefly, cells were plated at a density of 300×10^3 cells per dish on poly-L-lysine–coated coverslips. Coverslips were maintained in a 3% serum-containing Neurobasal medium (Thermo Fisher Scientific Inc., Waltham, USA). After 3 days in vitro (DIV), this initial plating medium was replaced by serum-free Neurobasal medium. Cultures were maintained at 37°C in 5% CO_2 for a maximum of 16 DIV. Single-particle (quantum dot) labeling and microscopy were performed as previously described (*20*). Briefly, dissociated cortical neurons at 14 to 16 DIV were first incubated for 10 min with rabbit polyclonal antibodies against the endogenous GluN2B NMDAR subunit (catalog number: AGC-003; 1:400; epitope corresponding to residues 323 to 337 of GluN2B; Alomone Labs, Jerusalem, Israel), washed, and then incubated for 10 min with F(ab')2-goat anti-rabbit IgG (H + L) secondary antibody, Qdot 655 (RRID:AB_1500763; catalog number: Q11422MP; 1:25 000; Thermo

Fisher Scientific Inc., Waltham, USA). All incubations were performed in preheated Tyrode solution [in mM: 105 NaCl, 5 KCl, 2 $MgCl_2$, 2 $CaCl_2$, 12 D-glucose, 25 Hepes (pH 7.4)] supplemented with 1% BSA (catalog number: A9647; Sigma-Aldrich, L'Isle D'Abeau Chesnes, France) to prevent unspecific binding. Green Mitotracker (catalog number: M7514; 1:2000 for 30 s; Thermo Fisher Scientific Inc., Waltham, USA) was used as endogenous synaptic marker. Quantum dots were visualized using a mercury lamp illumination, appropriate excitation/emission filters, and an EMCCD camera (EvolveTM, Teledyne Photometrics, Birmingham, UK). Images were acquired from randomly selected dendritic regions with an exposure time of 50 ms (20-Hz rate) for a duration of 500 consecutive frames. Recording sessions were processed with Metamorph (Molecular Devices). The instantaneous diffusion coefficient, D, was calculated for each trajectory from linear fits of the first 4 points of the MSD versus time function using the following formula: $MSD(t) = <r2> (t) = 4Dt$ (fig. S20A). The two-dimensional trajectories of single molecules in the plane of focus were constructed by correlation analysis between consecutive images using a Vogel algorithm.

Antibody-based x-link of NMDARs

Prevention of NMDAR surface redistributions was achieved using an antibody-based x-link strategy in which cultured hippocampal neurons were exposed for 30 min to high concentrations (0.08 mg/ml) of rabbit polyclonal immunoglobulins directed against extracellular epitopes of GluN2B subunits (RRID:AB_2040028; catalog number: AGC-003, Alomone Labs; epitopes corresponding to residues 323-337 of the GluN2B subunit, Jerusalem, Israel) to aggregate the receptors and limit their movements within the membrane plane, as previously described Fig. 6 and figs. S17 to S21) (*20*). The same strategy was also applied in vivo by injecting 0.8 µl of anti-GluN2B same as above) or anti-GluN2A (RRID:AB_2040025; Alomone Labs; epitope corresponding to residues 41 to 53 of GluN2A subunit, Jerusalem, Israel) antibodies (0.4 µg/ml in aCSF for each antibody) in the OFC at a rate of 0.6 µl/min. Injection of a goat anti-rabbit (0.4 µg/ml in aCSF; RRID: AB_11214051; catalog number: AP132, Millipore, Molsheim, France) was used as control.

Study design

We chose the sample size for each experiment based on previously published findings for which differences were achieved (*9*, *20*) and in accordance with the 3Rs principle. For in vivo and in vitro studies, rats or neuronal cultures were randomly assigned to the different treatment groups. Experiments were not always blinded because of lack of available experimenters with required expertise and to reduce the potential stress of rats exposed to a different experimenter.

Expression of data and statistical analyses

Results were expressed as means ± SEM unless otherwise stated. Data analyses were performed using analyses of variance (ANOVAs) followed by post hoc paired comparisons using Newman-Keuls F tests or Student's t tests where appropriate (GraphPad Prism version 9.5.1, USA). Values of $P < 0.05$ were considered as significant. Comparisons between distributions were performed using a Kolmogorov-Smirnov test. Single-particle tracking data such as instantaneous diffusion coefficients ($\mu m^2/s$) and surfaces explored ($\mu m^2/100$ ms) did not follow Gaussian distributions and were thus represented as median ± 25 to 75% interquartile range and assessed for statistical significance using a nonparametric test (Mann-Whitney test).

Supplementary Materials

The PDF file includes:

Figs. S1 to S21
Legend for data S1
References

Other Supplementary Material for this manuscript includes the following:

Data S1

REFERENCES AND NOTES

1. L. R. Squire, P. Alvarez, Retrograde amnesia and memory consolidation: A neurobiological perspective. *Curr. Opin. Neurobiol.* **5**, 169–177 (1995).
2. Y. Dudai, The neurobiology of consolidations, or, how stable is the engram? *Annu. Rev. Psychol.* **55**, 51–86 (2004).
3. S.-H. Wang, R. G. M. Morris, Hippocampal-neocortical interactions in memory formation, consolidation, and reconsolidation. *Annu. Rev. Psychol.* **61**, 49–79 (2010).
4. K. Takehara-Nishiuchi, Neurobiology of systems memory consolidation. *Eur. J. Neurosci.* **54**, 6850–6863 (2021).
5. P. W. Frankland, B. Bontempi, The organization of recent and remote memories. *Nat. Rev. Neurosci.* **6**, 119–130 (2005).
6. S. A. Josselyn, S. Tonegawa, Memory engrams: Recalling the past and imagining the future. *Science* **367**, eaaw4325 (2020).
7. A. P. Yiu, V. Mercaldo, C. Yan, B. Richards, A. J. Rashid, H.-L. L. Hsiang, J. Pressey, V. Mahadevan, M. M. Tran, S. A. Kushner, M. A. Woodin, P. W. Frankland, S. A. Josselyn, Neurons are recruited to a memory trace based on relative neuronal excitability immediately before training. *Neuron* **83**, 722–735 (2014).
8. M. Pignatelli, T. J. Ryan, D. S. Roy, C. Lovett, L. M. Smith, S. Muralidhar, S. Tonegawa, Engram cell excitability state determines the efficacy of memory retrieval. *Neuron* **101**, 274–284.e5 (2019).
9. E. Lesburguères, O. L. Gobbo, S. Alaux-Cantin, A. Hambucken, P. Trifilieff, B. Bontempi, Early tagging of cortical networks is required for the formation of enduring associative memory. *Science* **331**, 924–928 (2011).
10. N. M. Roüast, M. Schönauer, Continuously changing memories: A framework for proactive and non-linear consolidation. *Trends Neurosci.* **46**, 8–19 (2023).
11. M. Moscovitch, A. Gilboa, Has the concept of systems consolidation outlived its usefulness? Identification and evaluation of premises underlying systems consolidation. *Fac. Rev.* **11**, 33 (2022).
12. J.-H. Choi, S.-E. Sim, J.-I. Kim, D. I. Choi, J. Oh, S. Ye, J. Lee, T. Kim, H.-G. Ko, C.-S. Lim, B.-K. Kaang, Interregional synaptic maps among engram cells underlie memory formation. *Science* **360**, 430–435 (2018).
13. J.-H. Lee, W. B. Kim, E. H. Park, J.-H. Cho, Neocortical synaptic engrams for remote contextual memories. *Nat. Neurosci.* **26**, 259–273 (2023).
14. W. C. Abraham, A. Robins, Memory retention–The synaptic stability versus plasticity dilemma. *Trends Neurosci.* **28**, 73–78 (2005).
15. S. Fusi, P. J. Drew, L. F. Abbott, Cascade models of synaptically stored memories. *Neuron* **45**, 599–611 (2005).
16. P. Paoletti, C. Bellone, Q. Zhou, NMDA receptor subunit diversity: Impact on receptor properties, synaptic plasticity and disease. *Nat. Rev. Neurosci.* **14**, 383–400 (2013).
17. L. Groc, D. Choquet, Linking glutamate receptor movements and synapse function. *Science* **368**, eaay4631 (2020).
18. M. Potier, F. Georges, L. Brayda-Bruno, L. Ladépêche, V. Lamothe, A. S. Al Abed, L. Groc, A. Marighetto, Temporal memory and its enhancement by estradiol requires surface dynamics of hippocampal CA1 N-methyl-D-aspartate receptors. *Biol. Psychiatry* **79**, 735–745 (2015).
19. A. C. Gambrill, A. Barria, NMDA receptor subunit composition controls synaptogenesis and synapse stabilization. *Proc. Natl. Acad. Sci. U.S.A.* **108**, 5855–5860 (2011).
20. J. P. Dupuis, L. Ladépêche, H. Seth, L. Bard, J. Varela, L. Mikasova, D. Bouchet, V. Rogemond, J. Honnorat, E. Hanse, L. Groc, Surface dynamics of GluN2B-NMDA receptors controls plasticity of maturing glutamate synapses. *EMBO J.* **33**, 842–861 (2014).
21. M.-C. Lee, R. Yasuda, M. D. Ehlers, Metaplasticity at single glutamatergic synapses. *Neuron* **66**, 859–870 (2010).
22. B. A. Richards, P. W. Frankland, The persistence and transience of memory. *Neuron* **94**, 1071–1084 (2017).
23. B. G. Galef, A case study in behavioral analysis, synthesis and attention to detail: Social learning of food preferences. *Behav. Brain Res.* **231**, 266–271 (2012).
24. G. Schoenbaum, M. Roesch, Orbitofrontal cortex, associative learning, and expectancies. *Neuron* **47**, 633–636 (2005).
25. R. P. Kesner, The posterior parietal cortex and long-term memory representation of spatial information. *Neurobiol. Learn. Mem.* **91**, 197–206 (2009).
26. B. G. Galef, J. R. Mason, G. Preti, N. J. Bean, Carbon disulfide: A semiochemical mediating socially-induced diet choice in rats. *Physiol. Behav.* **42**, 119–124 (1988).

27. B. Bessières, O. Nicole, B. Bontempi, Assessing recent and remote associative olfactory memory in rats using the social transmission of food preference paradigm. *Nat. Protoc.* **12**, 1415–1436 (2017).
28. T. Kawashima, H. Okuno, M. Nonaka, A. Adachi-Morishima, N. Kyo, M. Okamura, S. Takemoto-Kimura, P. F. Worley, H. Bito, Synaptic activity-responsive element in the Arc/Arg3.1 promoter essential for synapse-to-nucleus signaling in activated neurons. *Proc. Natl. Acad. Sci. U.S.A.* **106**, 316–321 (2009).
29. L. Nadel, A. Hupbach, R. Gomez, K. Newman-Smith, Memory formation, consolidation and transformation. *Neurosci. Biobehav. Rev.* **36**, 1640–1645 (2012).
30. H. Lehmann, F. T. Sparks, S. C. Spanswick, C. Hadikin, R. J. McDonald, R. J. Sutherland, Making context memories independent of the hippocampus. *Learn. Mem.* **16**, 417–420 (2009).
31. A. J. Rashid, C. Yan, V. Mercaldo, H.-L. L. Hsiang, S. Park, C. J. Cole, A. de Cristofaro, J. Yu, C. Ramakrishnan, S. Y. Lee, K. Deisseroth, P. W. Frankland, S. A. Josselyn, Competition between engrams influences fear memory formation and recall. *Science* **353**, 383–387 (2016).
32. D. J. Cai, D. Aharoni, T. Shuman, J. Shobe, J. Biane, W. Song, B. Wei, M. Veshkini, M. La-Vu, J. Lou, S. E. Flores, I. Kim, Y. Sano, M. Zhou, K. Baumgaertel, A. Lavi, M. Kamata, M. Tuszynski, M. Mayford, P. Golshani, A. J. Silva, A shared neural ensemble links distinct contextual memories encoded close in time. *Nature* **534**, 115–118 (2016).
33. S. A. Josselyn, P. W. Frankland, Memory allocation: Mechanisms and function. *Annu. Rev. Neurosci.* **41**, 389–413 (2018).
34. R. J. Steele, R. G. Morris, Delay-dependent impairment of a matching-to-place task with chronic and intrahippocampal infusion of the NMDA-antagonist D-AP5. *Hippocampus* **9**, 118–136 (1999).
35. K. Takehara-Nishiuchi, S. Kawahara, Y. Kirino, NMDA receptor-dependent processes in the medial prefrontal cortex are important for acquisition and the early stage of consolidation during trace, but not delay eyeblink conditioning. *Learn. Mem.* **12**, 606–614 (2005).
36. J. Lisman, Criteria for identifying the molecular basis of the engram (CaMKII, PKMzeta). *Mol. Brain* **10**, 55 (2017).
37. F. Gardoni, MAGUK proteins: New targets for pharmacological intervention in the glutamatergic synapse. *Eur. J. Pharmacol.* **585**, 147–152 (2008).
38. M. P. Lussier, A. Sanz-Clemente, K. W. Roche, Dynamic regulation of N-methyl-d-aspartate (NMDA) and α-amino-3-hydroxy-5-methyl-4-isoxazolepropionic Acid (AMPA) receptors by posttranslational modifications. *J. Biol. Chem.* **290**, 28596–28603 (2015).
39. D. H. Han, P. Park, D. I. Choi, T. V. P. Bliss, B.-K. Kaang, The essence of the engram: Cellular or synaptic? *Semin. Cell Dev. Biol.* **125**, 122–135 (2022).
40. R. A. W. Frank, N. H. Komiyama, T. J. Ryan, F. Zhu, T. J. O'Dell, S. G. N. Grant, NMDA receptors are selectively partitioned into complexes and supercomplexes during synapse maturation. *Nat. Commun.* **7**, 11264 (2016).
41. S. Strack, R. J. Colbran, Autophosphorylation-dependent targeting of calcium/calmodulin-dependent protein kinase II by the NR2B subunit of the *N* -methyl- d-aspartate receptor. *J. Biol. Chem.* **273**, 20689–20692 (1998).
42. A. S. Leonard, I. A. Lim, D. E. Hemsworth, M. C. Horne, J. W. Hell, Calcium/calmodulin-dependent protein kinase II is associated with the N-methyl-D-aspartate receptor. *Proc. Natl. Acad. Sci. U.S.A.* **96**, 3239–3244 (1999).
43. W. Tao, J. Lee, X. Chen, J. Díaz-Alonso, J. Zhou, S. Pleasure, R. A. Nicoll, Synaptic memory requires CaMKII. *eLife* **10**, e60360 (2021).
44. A. R. Halt, R. F. Dallapiazza, Y. Zhou, I. S. Stein, H. Qian, S. Juntti, S. Wojcik, N. Brose, A. J. Silva, J. W. Hell, CaMKII binding to GluN2B is critical during memory consolidation. *EMBO J.* **31**, 1203–1216 (2012).
45. T. Rossetti, S. Banerjee, C. Kim, M. Leubner, C. Lamar, P. Gupta, B. Lee, R. Neve, J. Lisman, Memory erasure experiments indicate a critical role of CaMKII in memory storage. *Neuron* **96**, 207–216.e2 (2017).
46. R. Yasuda, Y. Hayashi, J. W. Hell, CaMKII: A central molecular organizer of synaptic plasticity, learning and memory. *Nat. Rev. Neurosci.* **23**, 666–682 (2022).
47. F. El Gaamouch, A. Buisson, O. Moustie, M. Lemieux, S. Labrecque, B. Bontempi, P. De Koninck, O. Nicole, Interaction between CaMKII and GluN2B controls ERK-dependent plasticity. *J. Neurosci.* **32**, 10767–10779 (2012).
48. B. Kellermayer, J. S. Ferreira, J. Dupuis, F. Levet, D. Grillo-Bosch, L. Bard, J. Linarès-Loyez, D. Bouchet, D. Choquet, D. A. Rusakov, P. Bon, J.-B. Sibarita, L. Cognet, M. Sainlos, A. L. Carvalho, L. Groc, Differential nanoscale topography and functional role of GluN2-NMDA receptor subtypes at glutamatergic synapses. *Neuron* **100**, 106–119.e7 (2018).
49. K. Yashiro, B. D. Philpot, Regulation of NMDA receptor subunit expression and its implications for LTD, LTP, and metaplasticity. *Neuropharmacology* **55**, 1081–1094 (2008).
50. P. Rao-Ruiz, E. Visser, M. Mitrić, A. B. Smit, M. C. van den Oever, A synaptic framework for the persistence of memory engrams. *Front. Synaptic Neurosci.* **13**, 661476 (2021).
51. J. V. Gallinaro, N. Gašparović, S. Rotter, Homeostatic control of synaptic rewiring in recurrent networks induces the formation of stable memory engrams. *PLOS Comput. Biol.* **18**, e1009836 (2022).
52. O. A. Shipton, O. Paulsen, GluN2A and GluN2B subunit-containing NMDA receptors in hippocampal plasticity. *Philos. Trans. R. Soc. B* **369**, 20130163 (2014).
53. E. Loftus, Our changeable memories: Legal and practical implications. *Nat. Rev. Neurosci.* **4**, 231–234 (2003).
54. W. Mau, M. E. Hasselmo, D. J. Cai, The brain in motion: How ensemble fluidity drives memory-updating and flexibility. *eLife* **9**, e63550 (2020).
55. Y. Dudai, A. Karni, J. Born, The consolidation and transformation of memory. *Neuron* **88**, 20–32 (2015).
56. M. Moscovitch, R. Cabeza, G. Winocur, L. Nadel, Episodic memory and beyond: The hippocampus and neocortex in transformation. *Annu. Rev. Psychol.* **67**, 105–134 (2016).
57. J. Lisman, R. Morris, Why is the cortex a slow learner? *Nature* **411**, 248–249 (2001).
58. D. Tse, R. F. Langston, M. Kakeyama, I. Bethus, P. A. Spooner, E. R. Wood, M. P. Witter, R. G. M. Morris, Schemas and memory consolidation. *Science* **316**, 76–82 (2007).
59. R. L. Davis, Y. Zhong, The biology of forgetting–A perspective. *Neuron* **95**, 490–503 (2017).
60. J. H. Jung, Y. Wang, A. J. Mocle, T. Zhang, S. Köhler, P. W. Frankland, S. A. Josselyn, Examining the engram encoding specificity hypothesis in mice. *Neuron* **15**, S854 (2023).
61. T. Kitamura, S. K. Ogawa, D. S. Roy, T. Okuyama, M. D. Morrissey, L. M. Smith, R. L. Redondo, S. Tonegawa, Engrams and circuits crucial for systems consolidation of a memory. *Science* **356**, 73–78 (2017).
62. T. J. Teyler, J. W. Rudy, The hippocampal indexing theory and episodic memory: Updating the index. *Hippocampus* **17**, 1158–1169 (2007).
63. G. M. Wittenberg, J. Z. Tsien, An emerging molecular and cellular framework for memory processing by the hippocampus. *Trends Neurosci.* **25**, 501–505 (2002).
64. E. G. Hughes, X. Peng, A. J. Gleichman, M. Lai, L. Zhou, R. Tsou, T. D. Parsons, D. R. Lynch, J. Dalmau, R. J. Balice-Gordon, Cellular and synaptic mechanisms of anti-NMDA receptor encephalitis. *J. Neurosci.* **30**, 5866–5875 (2010).
65. J. G. Klinzing, N. Niethard, J. Born, Mechanisms of systems memory consolidation during sleep. *Nat. Neurosci.* **22**, 1598–1610 (2019).
66. C. Kilkenny, W. J. Browne, I. C. Cuthill, M. Emerson, D. G. Altman, Improving bioscience research reporting: The ARRIVE guidelines for reporting animal research. *PLOS Biol.* **8**, 5 (2010).
67. P. Alvarez, P. A. Lipton, R. Melrose, H. Eichenbaum, Differential effects of damage within the hippocampal region on memory for a natural, nonspatial odor-odor association. *Learn. Mem.* **8**, 79–86 (2001).
68. R. E. Clark, N. J. Broadbent, S. M. Zola, L. R. Squire, Anterograde amnesia and temporally graded retrograde amnesia for a nonspatial memory task after lesions of hippocampus and subiculum. *J. Neurosci.* **22**, 4663–4669 (2002).
69. A. J. Milnerwood, C. M. Gladding, M. A. Pouladi, A. M. Kaufman, R. M. Hines, J. D. Boyd, R. W. Y. Ko, O. C. Vasuta, R. K. Graham, M. R. Hayden, T. H. Murphy, L. A. Raymond, Early increase in extrasynaptic NMDA receptor signaling and expression contributes to phenotype onset in huntington's disease mice. *Neuron* **65**, 178–190 (2010).
70. O. Nicole, D. M. Bell, T. Leste-Lasserre, H. Doat, F. Guillemot, E. Pacary, CaMKIIβ regulates nucleus-centrosome coupling in locomoting neurons of the developing cerebral cortex. *Mol. Psychiatry* **23**, 2111 (2018).
71. G. Paxinos, C. Watson, *The rat brain in stereotaxic coordinates* (Academic Press, 1998).
72. M. F. Nambu, Y.-J. Lin, J. Reuschenbach, K. Z. Tanaka, What does engram encode?: Heterogeneous memory engrams for different aspects of experience. *Curr. Opin. Neurobiol.* **75**, 102568 (2022).
73. A. Goto, A. Bota, K. Miya, J. Wang, S. Tsukamoto, X. Jiang, D. Hirai, M. Murayama, T. Matsuda, T. J. McHugh, T. Nagai, Y. Hayashi, Stepwise synaptic plasticity events drive the early phase of memory consolidation. *Science* **374**, 857–863 (2021).
74. J. D. Carvalho-Rosa, N. C. Rodrigues, A. Silva-Cruz, S. H. Vaz, D. Cunha-Reis, Epileptiform activity influences theta-burst induced LTP in the adult hippocampus: A role for synaptic lipid raft disruption in early metaplasticity? *Front. Cell. Neurosci.* **17**, 1117697 (2023).

Acknowledgments: We thank the IINS Cell Biology facility, especially E. Verdier, L. Villetelle, and D. Bouchet, for molecular and cellular tool productions. Microscopy was done at the Bordeaux Imaging Center, a CNRS-INSERM, and Bordeaux University service unit, a member of the national infrastructure France BioImaging. We are grateful to E. Pacary for cloning and production of molecular biology tools, A. Hambucken for validation of behavioral paradigms, and C. Duffau for imaging analysis. We are also grateful to members of the Bontempi and Groc laboratories for stimulating discussions. **Funding:** This work was financially supported by the Fondation pour la Recherche Médicale (FRM-DEQ20130326468 to B.Bo.), the Fondation France Alzheimer and Fondation de France (to B.Bo.), the Agence Nationale pour la Recherche (ANR-14-CE13-0017-01, project MemoryTrack to B.Bo.), the Agence Nationale pour la Recherche (ANR-22-CE16-0026, project GrinTrack to O.N.), the CNRS and the University of Bordeaux (UMR 5293, UMR 5287 and UMR 5297), and Labex Brain fellowship (PhD extension program, B.Be.). B.Bo, L.G., and O.N. received financial support from the French government in the framework of the University of Bordeaux's IdEx "Investments for the Future" program (GPR BRAIN_2030). **Author contributions:** Conceptualization: B.Be., B.Bo., and O.N. Methodology:

B.Be., J.D., L.G., B.Bo., and O.N. Investigation: B.Be., J.D., L.G., B.Bo., and O.N. Resources: L.G., B.Bo., and O.N. Data curation: L.G. and O.N. Formal analysis: B.Be., J.D., L.G., B.Bo., and O.N. Software: L.G. Validation: B.Be., J.D., L.G., B.Bo., and O.N. Visualization: B.Be., J.D., B.Bo., and O.N. Funding acquisition: L.G., B.Bo., and O.N. Project administration: B.Bo. and O.N. Supervision: B.Bo. and O.N. Writing—original draft: B.Bo. and O.N. Writing—review and editing: B.Be., J.D., L.G., B.Bo., and O.N. **Competing interests:** The authors declare that they have no competing interests. **Data and materials availability:** All data needed to evaluate the conclusions in the paper are present in the paper and/or the Supplementary Materials. Raw data, including complete statistics tables, are available in data S1 file.

Submitted 18 January 2024
Accepted 26 July 2024
Published 30 August 2024
10.1126/sciadv.ado1148